JOURNAL OF MATERIALS SCIENCE 18 (1983) 3311–3322

Hot alkali stable materials with low electrical resistance: a new composite made from porous asbestos and soluble polyphenylene sulphide

E. MONTONERI*, L. GIUFFRÉ, G. MODICA, M. GENNUSO
Dipartimento di Chimica Industriale e Ingegneria Chimica del Politecnico di Milano, P.zza L. da Vinci 32, 20133 Milano, Italia

Dissolving *p*-polyphenylene sulphide (Ryton^R) at high concentrations (15 to 25 wt %) in diphenyl sulphide is the key factor to obtain Canadian crysotyle asbestos cardboard (0.055 cm thick) coated with variable amounts (7 to 22 wt %) of the organic polymer. Relative to known coating processes with PPS the use of concentrated polyphenylene sulphide solutions is quite new and yields stabilized asbestos materials whose physical, chemical structure and properties may be modified at will depending on the content of the organic polymer. These products have much higher mechanical strength and chemical stability in boiling 30 to 43 wt % KOH than the plain cardboard. Also due to the low electrical resistance (0.1 $\Omega\,cm^2$ at $T \geqslant 100°$ C) in 30 to 43% KOH they appear most suitable for testing in advanced alkaline water electrolysers. The mechanism of stabilization of asbestos by the organic polymer and the structure and chemical–physical behaviour of the plain and coated cardboard are discussed in the light of X-ray, SEM and IR data.

1. Introduction

The identification of stable and electrically conductive materials to work in hot ($T \geqslant 120°$ C) concentrated alkali (KOH 30 wt %) is a prior objective of advanced alkaline water electrolysis technology [1]. Traditional asbestos separators fail [2] at $T > 100°$ C due to insufficient mechanical strength and chemical deterioration with concomitant silicon leaching:

$$Mg_3Si_2O_5(OH)_4 + KOH(aq) = 3Mg(OH)_2 + \text{soluble silicates (aq)}. \quad (1)$$

Any new material should be physically and chemically more stable than asbestos, provide necessary mechanical strength and flexibility, and exhibit a surface specific electrical resistance not greater than 0.2 $\Omega\,cm^2$ [3]. Although several inorganic and organic alternatives to asbestos are currently being investigated [2, 4], much work is still being done on asbestos since the stabilization of this material remains mostly desirable.

Attempts to obtain stabilized asbestos [2], either by manufacturing mats with KOH leached fibres or adding other inorganic materials (TiO_2, or ZrO_2, or thin hydrosol), have been unsuccessful. We have found that coating asbestos cardboards with polyphenylene sulphide (PPS), $-C_6H_4-S-_n$, yields a new material which retains the desirable properties of both asbestos and PPS such as the porosity, wettability and flexibility of the former and the high chemical and mechanical stability of the latter [5].

2. Experimental procedure

2.1. Materials preparation

The manufacture† of the PPS–asbestos cardboard has been accomplished by soaking commercial

*To whom correspondence should be addressed.
†Preliminary communication given [6].

0022–2461/83 $03.00 + .12

(APC-CAT, Milan) Canadian crysotyle asbestos cardboards (0.055 cm thick), previously dried at 120° C for 24 h, with *p*-polyphenylene sulphide (Phillips Petroleum Co. Ryton^{R}) dissolved in BDH diphenyl sulphide (DPhS) at 220° C for 1/2 h, withdrawing the cardboard from the soaking bath, dripping and washing off the excess solvent with C. Erba RPE CS_2 at room temperature and drying the end product at 120° C for 24 h.

The amount of sorbed PPS was determined by the cardboard weight gain after soaking and drying and referred to the final overall weight to yield the wt% PPS concentration (C_1) in the end product. With this procedure C_1 depends on the initial concentration (C_2 wt%) of PPS in DPhS according to the empirical equation $C_1 = ZC_2$. No detailed work has been carried out to define the dependence of Z on experimental parameters, although Z values in the 0.44 to 0.74 range were obtained on changing the specimen size (from 9 to 100 cm^2) and the capacity of the soaking reactor.

The imbibition of the cardboards was carried out in cylindrical glass reactors which comprise a lower zone, heated by an electrical mantle and magnetically stirred, and an upper jacketed zone for circulation of room temperature water. The reactor head, which is either inserted through ground cones or clamped to the reactor body, contains a cylindrical central inlet to feed the solid PPS into the solvent heated zone and refrigerating coil around the solid inlet down to the lower end of the jacketed reactor zone. This assembly is required to minimize costly solvent evaporation losses and keep constant PPS concentrations during operation.

After achieving complete dissolution of the required amount of PPS in the solvent, the reactor head is removed temporarily and a set of cardboards, held vertically into a glass cage, is inserted down into the PPS solution. The sample holder is made by 4 vertical thin rods at right angles to each other and joined at both the upper and lower ends, respectively, by two horizontal and intercrossing staffs. After the required soaking time the reactor head is removed again and the cage withdrawn from the reactor. During this operation a vertical rather than horizontal sample arrangement in the soaking bath is preferred to avoid dripping of PPS drain solution from the upper to the lower cardboards and, on cooling, crystallization of excess PPS onto the cardboard surface.

On cooling the $C_2 \geqslant 8$ to 10 wt% soakings baths turn into a wet paste. Eventually the organic polymer and the solvent may be separated and re-used by washing the exhausted bath with benzene (or CS_2), drying the solid residue, and distilling off benzene from the collected washings. The presence of low boiling materials in the recovered DPhS and/or PPS cause bursting of the soaking bath and eventually decrease the PPS solubility. These materials may be removed by distillation, prior to the cardboard soaking, in the same imbibition reactor simply by properly increasing the temperature of the refrigerating fluid into the reactor upper zone.

2.2. Test of stability in hot concentrated alkali

The cardboard's stability in alkali was tested by exposing round specimen with 6 cm diameter to boiling concentrated (30 to 40 wt%) KOH for a maximum of 2700 h in teflon cylindrical vessels which are equipped with screw caps, glass reflux condensers and terminated by drierite CO_2 absorbers. The whole assembly is kept in a thermostatted oil bath. At the end of the test period the specimen was withdrawn from the potash, washed with deionized water to neutral pH and dried for 24 h at 120° C. The samples were compared to the initial specimen before exposure to the alkali ($t = 0$ h) and characterized (Tables I and II and Figs. 1 to 9) by their weight loss, chemical composition change (SiO_2, MgO and PPS wt%), X-ray and infrared (IR) spectra, SEM micrographs, water and toluene regains, tensile strength and electrical resistance in the concentrated alkali.

2.3. Characterization procedures and techniques

2.3.1. Electrical resistance

The ohmic drop (R_s, $\Omega\,cm^2$) across the separator was measured in a glass thermostatted electrolytic cell made of two separate cylindrical bodies (Fig. 1) clamped together in q and held in contact by silicon rubber gaskets (p). The head of each body is equippped with a vapour condenser (a) to minimize water evaporation loss, a ground cone to hold the gas evolving nickel electrode (c) and an electrolyte inlet (e). The lower part of each body contains an electrolyte outlet (l) near q and the exit to the by-pass (f) which is closed by the valve (g) during the measurement of the potential between the electrodes housed in (d) and allows intermixing of the cathodic and anodic electrolyte

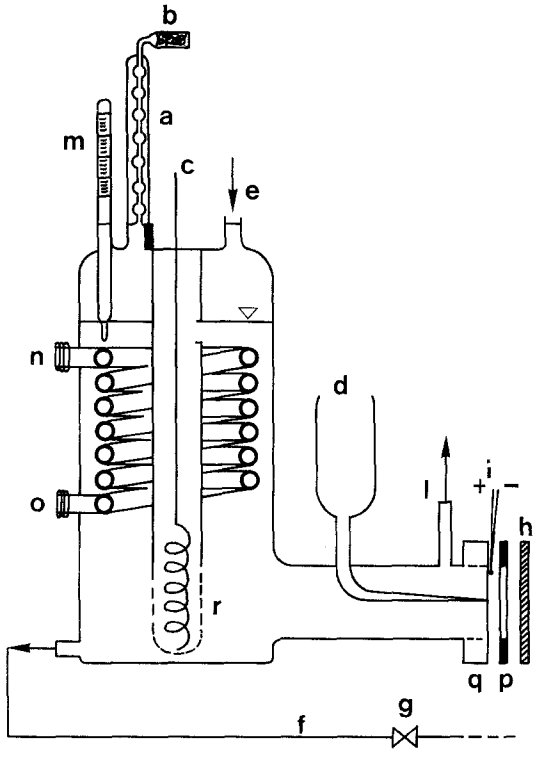

Figure 1 Experimental set-up for measuring the electrical resistance across the separator.

only between measurements. The electrolyte circulation in the system is maintained by a multichannel pump, even during the measurement of the potential, to minimize temperature gradients through the cell and to remove possible accumulation of gas bubbles near the separator (h) lodging. Also, for this last reason, the gas evolving electrode (nickel) is housed in (r) which terminates with a porous glass fritt. The potential measuring electrode (Hg/HgO/KOH) is housed in a reservoir (d) which is filled with the cell electrolyte and terminates with a lugging capillary near the separator lodging. The whole assembly is kept in a fixed position and inserted into the cell bodies by means of a group cone. The temperature is measured by the thermocouple (i) inserted in the vicinity of the separator lodging. The (d) potential (V) between the Hg/HgO electrodes, as a function of current densities (cd), is measured alternatively in the presence (V_p) and absence (V_a) of the separator. At any current density the latter value is substracted from the former. The net potential value (V_n) represents the amount of voltage drop due to the separator phase, since the electrodes' gap in presence of the separator increases by an amount equal to the separator thickness. All V against cd plots were linear (regression coefficients $\geqslant 0.999$) up to 0.7 A cm^{-2} cd values. The R_s values were calculated from the slopes of the V_n against cd linear regressions and were reproducible to ± 5% at the 95% confidence level.

2.3.2 SEM, X-rays and IR scans

SEM, X-ray and IR (on KBr discs obtained with previously ground and pulverized cardboards) scans were obtained with JSMU3, Philips PW1050 powder diffractometer and P.E. 157G and 457 instruments. The PPS wt% concentration, in the samples which had been exposed to the action of the alkali ($t > 0$ h), was determined by IR spectroscopy as discussed in the text.

2.3.3. SiO_2 and MgO analyses

The SiO_2 and MgO wt% concentrations were determined according to known wet chemical procedures by melting the pulverized cardboard with $NaHCO_3$ and running the mixture through three consecutive dissolution-drying cycles with diluted HCl and diluted and concentrated H_2SO_4, respectively. The residue, taken up with hot water and filtered, yields an insoluble part (i) and a filtrate (s). The insoluble residue (i) is calcined, weighed (to yield W_1), taken up with H_2O/HF, dried and reweighed (to yield W_2). The SiO_2 content is calculated from $W_2 - W_1$. The W_2 residue is taken up with HCl, mixed with the filtrate (s), added with H_2O_2 and ammonia to precipitate $MgNH_4PO_4$. This solid, after filtration, is calcined and weighed to yield the MgO content.

2.3.4. Weight regain

The liquids take up (g of sorbed liquid per g of dry cardboard) was determined, according to a known procedure [7] by equilibrating the specimen in either H_2O or toluene at room temperature for 24 h, withdrawing the specimen from the soaking bath, quickly blotting their surfaces with filter paper and weighing.

2.3.5. Tensile strength

The tear point pressure ($P_t = \text{kg cm}^{-2}$) was measured with DiE D 638, type I (ASTM 1970). The cardboard thickness, measured with a Kafer (Germany) micrometer, was constant (0.0550 ± 0.0005 cm) regardless of the PPS content (C_1). Both the plain and coated asbestos cardboards exhibited negligible stretching before tearing under a traction rate of 5 mm min^{-1}.

3. Results and discussion

3.1. Materials preparation

For the manufacture of PPS coated asbestos the following alternatives were considered:

(a) synthesis of the organic polymer directly into the asbestos host phase and

(b) coating asbestos with authentic PPS either in the melt state (b_1) or diluted into a proper solvent (b_2).

In all cases the chosen asbestos host matrix was in the form of porous cardboard to work on a preformed morphological structure typical of electrolytic separators. Following the guidelines of the procedure which we have reported previously for the manufacture of polystyrene–divinylbenzene (SDVB) coated asbestos cardboard [8], the *in situ* polymerization technique (a) involves soaking of the plain cardboard into a solution of the polymerization reagents, dripping off the excess solution and reacting the sorbed monomers–catalyst mixture into the asbestos phase.

For PPS this procedure proved unpractical since, unlike the SDVB case, the synthesis of the former [5, 9] occurs in drastic acid or alkaline experimental conditions which are critical for the host matrix structures [2, 10, 11]. The (b) procedure enables one to start from commercial polymers with known and controlled specifications, but requires that the organic polymer has a melting temperature compatible with the thermal stability of the host matrix or that it is soluble.

Unlike the SDVB case, PPS was found to meet both requirements. However the imbibition of the commercial asbestos cardboard with melted PPS ($T \geqslant 280^\circ$ C) was not successful since the former material exhibits some weight loss at $T > 250^\circ$ C and it is difficult to control the PPS concentration in the end product. The asbestos weight gain after soaking with melt PPS is very high (> 100%), but most of the organic polymer concentrates on the cardboard surfaces and yields very rigid structures. The problems with the b_2 procedure was to find a proper solvent for PPS which met the following requirements:

1. solubility temperature $\leqslant 250^\circ$ C and
2. PPS solubility (C_2) $\geqslant 10$ wt %.

At lower C_2 values the PPS content which penetrates into the asbestos phase does not sufficiently coat the asbestos fibres to achieve their stabilization. No solvent could be found which dissolved PPS at room temperature. Out of a number of high boiling solvents (aromatics, chlorinated aromatic, dialkylsulphides, diphenylsulphide and -disulphide) which were tried, diphenyl sulphide exhibited the most desirable characteristic since, by virtue of its structural identity with the PPS monomeric repeating unit, it was found to dissolve up to 25 wt % of PPS at 220° C, can be used in the liquid state in a wide temperature range (from −26 to 296° C) and may be separated from PPS and asbestos simply by dripping off at room temperature the solvent from the soaked carboard. The PPS solutions in DPhS penetrate well into the asbestos matrix and the organic polymer distributes uniformly into the cardboard structure. On withdrawing from the soaking bath (see experimental work) the asbestos surfaces appear darker than initially, but homogeneous and smooth, provided that the soaking bath does not contain undissolved PPS particles and vertical rather than horizontal cardboard arrangement is adopted. The overall structure of the soaked cardboards turns out to be more rigid than that of plain asbestos, but it is still so flexible that it can be bent from an initial diameter of 13 cm up to 8 cm without breaking.

The b_2 procedure is absolutely innovative in polyphenylene sulphide coating technology [5] which, due to the previously reported insolubility of PPS, has been restricted so far to the use of powders or aqueous slurries. The herein reported availability of concentrated PPS solutions* allows easy control of the final concentration (C_1) of sorbed PPS into the cardboard and, thus, to modify the properties of the end product at will.

3.2. Structural characterization and properties

3.2.1. Asbestos and asbestos–PPS as made

Basically the morphology, chemical composition and properties of the above manufactured PPS–asbestos cardboards turn out to be those which

*The technological implications of the PPS solubility are much wider than those related to the coating of asbestos cardboards. It has been found in fact that coatings of PPS may be applied to metals and to any porous matrix. For instance, in the same experimental conditions, carbon felts adsorb two or three times more PPS than the asbestos cardboard does, depending on the relative porosity. Also starting from fibres, materials in the form of diaphragms or membranes may be obtained on cooling slurries of fibres in hot DPhS–PPS solutions. Finally films of PPS, neat or together with other polymers soluble in the same solvent, may be obtained by known solution casting procedures [12, 13].

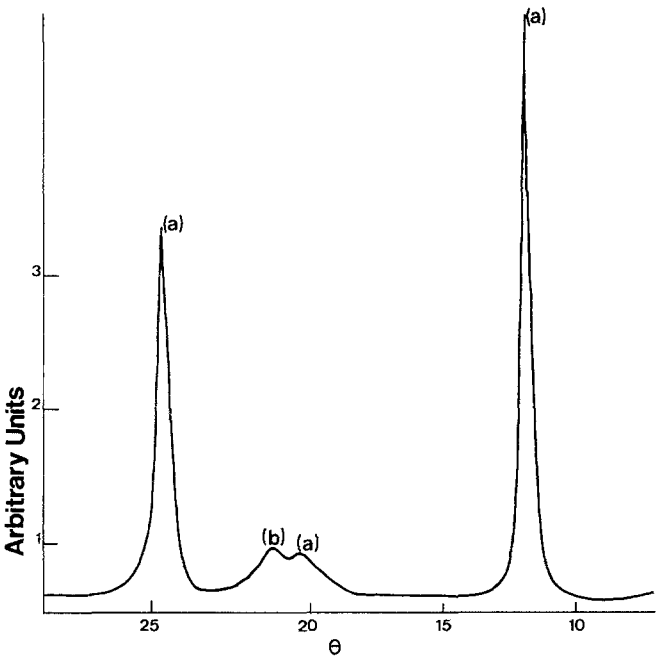

Figure 2 Asbestos (a) and PPS (b) X-ray powder diffraction patterns in the 11.5 wt% PPS–asbestos cardboard: θ = Bragg angle.

may be accounted for by a physical mixture of crysotyle asbestos and PPS in which the chemical identity of the neat materials remains unaltered at the end of the soaking process. The MgO/SiO_2 mole ratio of the asbestos matrix in the PPS–asbestos cardboards was found identical to that of the plain cardboard and corresponding to the known $Mg_3Si_2O_5$ [10, 11] stoichiometry. The X-ray diffraction patterns (Fig. 2) of the soaked PPS asbestos cardboards contain features which are identical to those of the starting authentic materials and show both compounds to be present in the cardboard in the same crystalline phase that they have in the neat state. The IR spectra exhibit characteristic absorption frequencies ($\nu\,cm^{-1}$ in Fig. 3) which are associated with the stretching vibrations of terminal hydroxyls (ν_{MO-H} 3662 [14]) and chain Si–O (ν_{Si-O} 955 [15–18]) bonds of the asbestos magnesium polysilicate structure [10, 11], with the sorbed water (ν_{H_2O} 3400 [19]) and with the bond vibrations of the aromatic polymer (ν_{PPS} 1572, 1468 and 1385). In this work the above bands are proven valuable to appreciate structural and chemical composition changes in the asbestos–PPS cardboards. The $1000 \leqslant \nu \leqslant 1100$ and $\nu \geqslant 810$ ranges are not as helpful due to the overlapping of the asbestos and PPS absorptions. Each polymer in the PPS–asbestos cardboards, and regardless of PPS concentration, is characterized by absorption frequencies and bands relative intensities which are identical to those of the corresponding neat material. Therefore, under these experimental conditions, no specific chemical interaction [20–23] between asbestos and PPS functional groups can be assessed. The most evident change in the IR spectra is related to the PPS

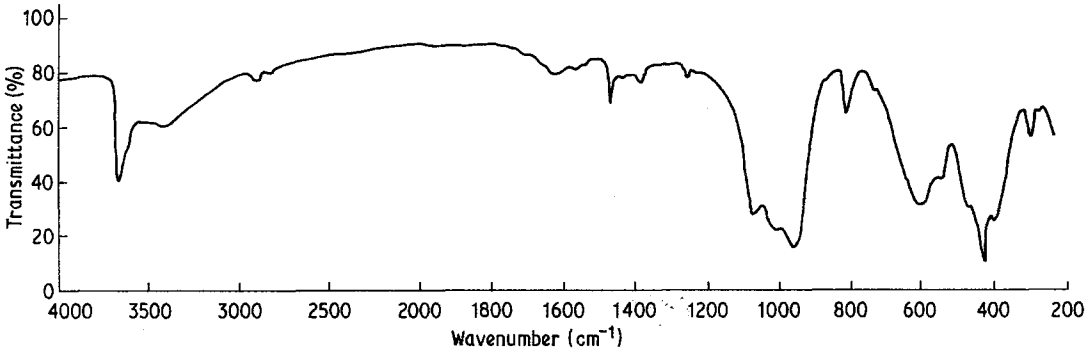

Figure 3 IR spectrum of Canadian commercial asbestos cardboard coated with 19 wt% PPS.

to asbestos bands intensity ratios (e.g. R_1 and R_2 equal to the 1468 to 3662 and 1468 to 955 cm^{-1} bands net absorbance ratios, respectively). Within the net absorbance (A_ν) ranges, $0.25 \leqslant A_{3662} - A_{3800} \leqslant 0.52$, $0.55 \leqslant A_{955} - A_{850} \leqslant 1.00$, and $0.08 \leqslant A_{1468} - A_{1500} \leqslant 0.13$, R_1 and R_2 increase linearly with the cardboard weight gain (C_1) after adsorption of PPS, according to

$$R_1 = a_1 C_1 \quad (2)$$

and

$$R_2 = a_2 C_2 \quad (3)$$

where $a_1 = (19 \pm 2.6) \times 10^{-3}$, $a_2 = (8.79 \pm 0.93) \times 10^{-3}$ and r (correlation coefficient) $\geqslant 0.97$.

The scanning electron micrographs of the plain asbestos cardboard (Fig. 4a) reveal the typical features of coarsely porous membranes with sponge structure and rather broad pore size distribution [13]. The micrographs of the PPS–asbestos cardboard (Fig. 4b) show a more compact structure characterized by highly dense areas, where very few and small, or no pores, are visible, separated by deep void channels. Also the individual bundles and network of asbestos fibres of Fig. 4a are not visible in Fig. 4b, although some filament ends appear casually to stick out of the compact areas.

Undoubtedly the adsorption of PPS by the porous asbestos matrix is mainly due to physical rather than chemical factors. During the cardboard soaking into the hot PPS solution the latter penetrates into the pores of the host framework. At lower temperature, the organic polymer crystallizes out of the DPhS solvent onto the polysilicate phase, thus coating the asbestos fibres and partially reducing the overall void fraction of the structure. The maximum take up of organic polymer by the asbestos cardboard certainly depends on the latter void fraction and on the solubility of the former into the solvent of choice. The highest weight gain which has been attained in this work is ca. 25 wt% due to the limited solubility (23 wt% at 220° C) of PPS in DPhS. With a different organic polymer (polystyrene–divinylbenzene copolymer [8]) a maximum weight gain of 43 wt% was attained.

Any expectation on the properties of the PPS–asbestos cardboards must be based on the fact that higher PPS concentrations affect not only the morphology (e.g. void fraction) and the physical properties of the material, but also its chemical nature. Particular attention should be given also to the hydrophile–lipophile balance (HLB) in the overall material.

Filling the void volume of the plain cardboard with the organic polymer yields a specimen of much higher mechanical strength (Fig. 5). The morphological change towards a less porous material is also responsible for the decrease of the liquid uptake by the cardboard with increasing PPS concentration (Fig. 6). However the different water and toluene regains at equal PPS concentration demonstrate that the liquid uptake is not solely governed by the physical dimensions of the porous absorbing structure and permeant molecules, but the interactions of these latter with the pore walls of the former are also very important. Whereas plain asbestos absorbs more water than toluene (X = sorbed water to toluene wt/wt ratio = 1.2), the PPS–asbestos materials exhibit opposite behaviour ($X = 0.5$ to 0.6) due to their more lipophilous nature.

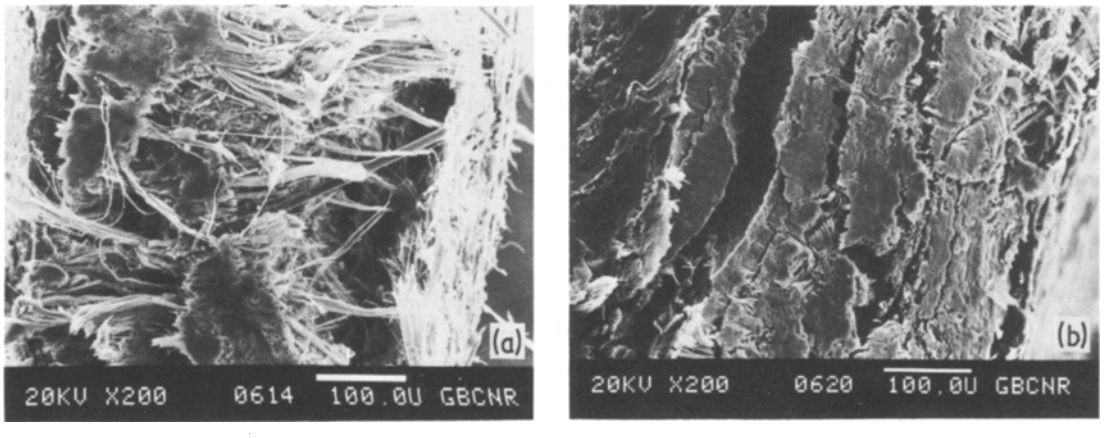

Figure 4 Cross-sectional SEM micrographs of asbestos cardboard (as made): (a) asbestos, (b) 11% PPS–asbestos.

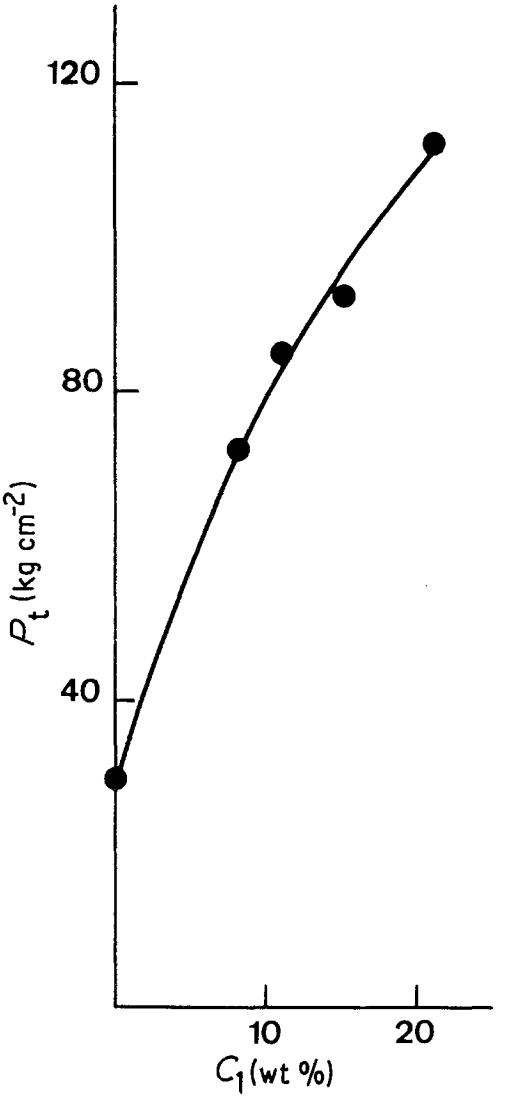

Figure 5 Tensile strength (P_t) of PPS–asbestos cardboards against PPS concentration (C_1).

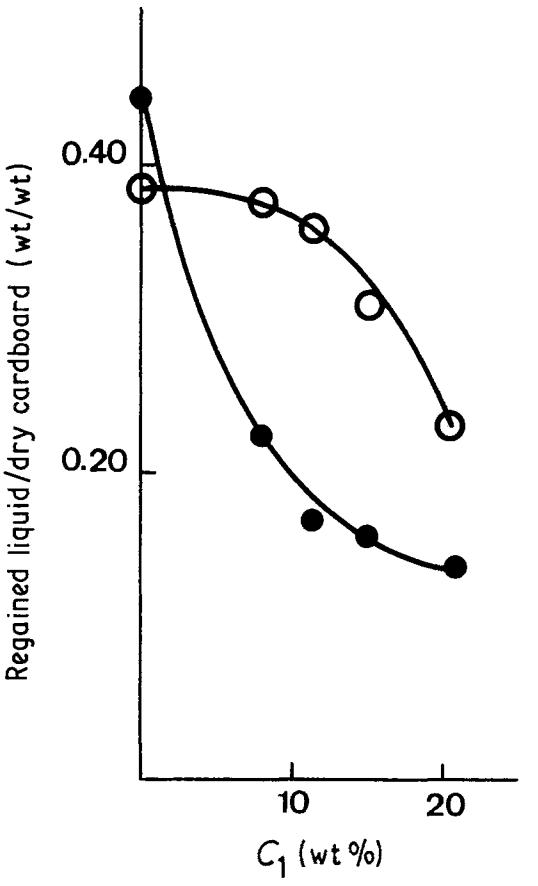

Figure 6 Liquids (•—water and ○—toluene) uptakes of PPS–asbestos cardboards against PPS concentration (C_1).

3.2.2. Asbestos and asbestos–PPS after exposure to boiling concentrated KOH

In as much as the specific application of this material in the field of alkaline water electrolysis is concerned, although the high mechanical strength is certainly desirable, excessive reduction of porosity and hydrophilicity is detrimental and expensive in terms of high voltage drop across the separator [4]. On this basis the materials containing between 6.5 and 11.5% PPS were selected to be studied further in relation to their behaviour in hot concentrated alkali since they exhibit a 2 to 3 fold higher mechanical strength than the plain cardboard and can still absorb between 25 and 18% water.

Table I shows that in the $t = 2700$ h plain card-

TABLE I MgO and SiO_2 concentration (wt/wt) and MOH/SiO IR bands absorbance ratios of plain and 11.4 wt % PPS–asbestos cardboards before ($t = 0$ h) and after ($t = 2700$ h) exposure to 30 wt % boiling KOH

Cardboard sample	t(h)	MgO (wt %)	SiO_2 (wt %)	MgO/SiO_2 (mole ratio)	MgO/$Mg_3Si_2O_5$* (mole ratio)	A_{955}/A_{3662}
Asbestos	0	34.24	34.16	1.5	0.0	2.01 ± 0.14
Asbestos	2700	45.13	12.76	5.3	7.6	0.58
11.4 wt/wt PPS–asbestos	0	31.82	29.48	1.6	0.2	2.01 ± 0.14
11.4 wt/wt PPS–asbestos	2700	33.85	25.06	2.0	1.0	1.66

*Calculated mole ratio based on the MgO content which has been found in excess over the $Mg_3Si_2O_5$ stoichiometry.

board the SiO_2 and MgO concentrations are, respectively, lower and higher than in the corresponding $t = 0$ h sample and the MgO/SiO_2 mole ratio in the former indicates the presence of a large excess of MgO over the stoichiometric requirement of the initial $Mg_3Si_2O_5$ composition. These data are in agreement with previous observations [2], based on Debye–Scherrer powder pattern, which indicate that the deterioration of asbestos in hot KOH (Reaction 1) leads to leaching of silicon from the asbestos and increasing concentration of brucite phase in the insoluble residue. Our IR spectra (Fig. 7) and SEM micrographs (Fig. 8) confirm this conclusion and reveal deep changes in the initial magnesium polysilicate structure which are related, respectively, to its chemical bonds distribution and morphology.

Contrary to the case of asbestos–PPS cardboards, for plain asbestos the entire IR absorption frequency range (Fig. 7) may be considered in more details since no interfering PPS bands are present. Although no specific work has been found in literature regarding definite band assignments in the IR spectra of crysotyle asbestos, from the knowledge on the vibrational modes of silicates SiO bonds [15–18] the absorption of the $t = 0$ h plain asbestos cardboard (Fig. 7a), which fall in the 1100 to 950, 600 and 500 to 400 cm^{-1} ranges, may be attributed to the Si–O–(Si) bonds asymmetric, symmetric stretching and bending vibrations, respectively. The broad absorption between 1070 and 950 cm^{-1} is due to the overlapping of three bands. The absorption maxima at 1070, 1010 and 955 cm^{-1} reveal a distribution of SiO_4 tetrahedra in the polysilicate chain back bone which differ one from the other in the bridging to non-bridging ($Si–O–Si/SiO^-$) oxygen ratios. The non-bridging oxygens may be terminated either by Mg^+ or H^+ ions to yield SiO–Mg and SiOH bonds. Whereas the stretching vibration of the terminal OH bonds yields a relatively sharp band at 3662 cm^{-1}, the Mg–O absorption is rather broad, covers the 300 to 600 cm^{-1} range [24] and contributes to the overall broadness of the spectrum in this region.

The spectrum of the plain asbestos cardboard after exposure to the hot alkali (Fig. 7b) exhibits quite different features. The net absorbance of the chain Si–O asymmetric stretching bands is drastically reduced relatively to that of the terminal OH functions (A_{955}/A_{3662} from 2.01 at $t = 0$ to 0.6–0.7 at $t = 200$ to 2700 h in Table II). Also the Si–O symmetric stretching and the bending vibration absorption maxima are not visible since they are totally covered by the typical Mg–O band [24]. The increase of terminal hydroxyl and

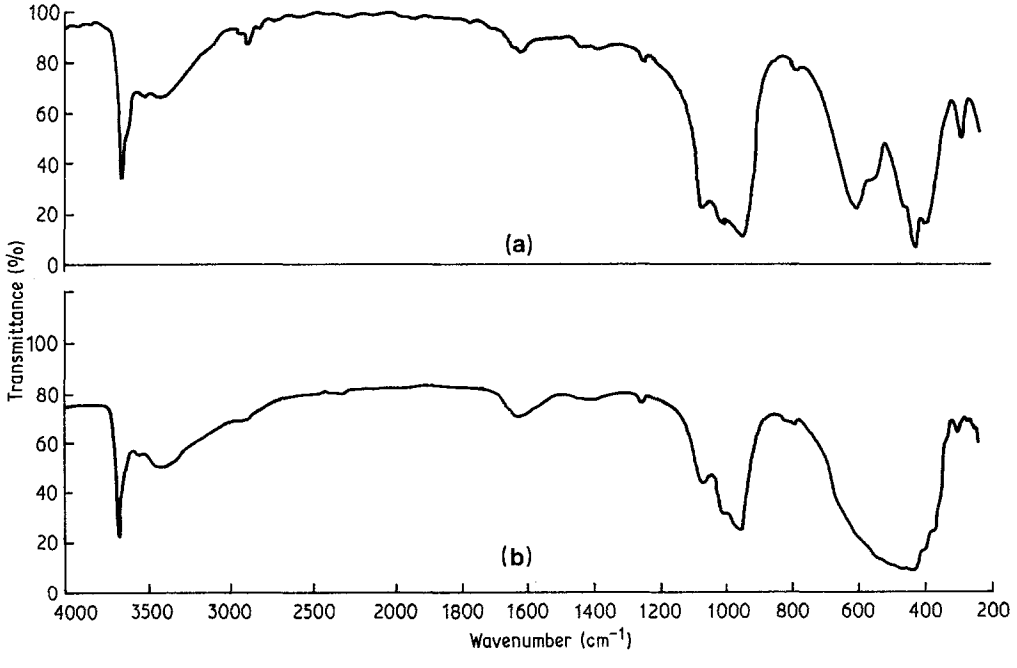

Figure 7 IR spectra of plain asbestos (a) before ($Mg_3Si_2O_5$) and (b) after ($MgO/Mg_3Si_2O_5 = 7.6$) 2700 h exposure to 30 wt % boiling KOH.

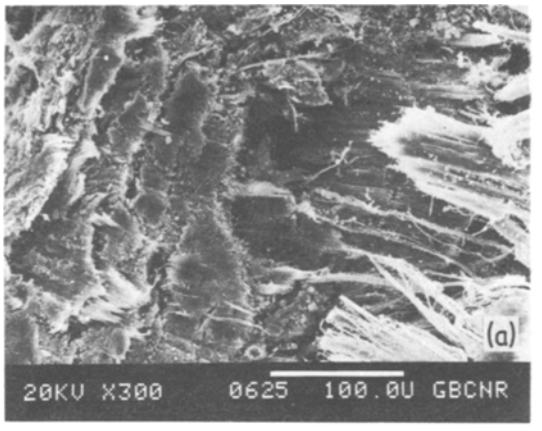

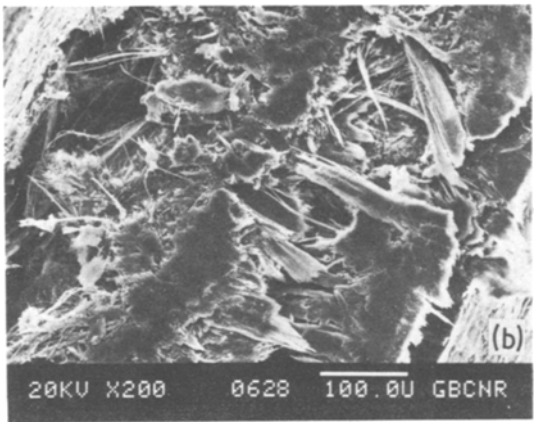

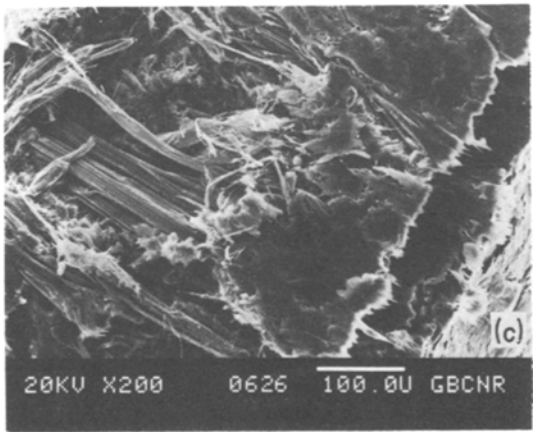

Figure 8 Cross-sectional SEM micrographs of asbestos cardboards after 2700 h exposure to 30 wt% boiling KOH: (a) plain, (b) and (c) 11 wt% PPS–asbestos.

Mg–O bonds at the expense of SiOSi bridges is well consistent with a considerable shift of Reaction 1 to the right.

The SEM micrograph of the plain asbestos $t = 2700$ h sample (Fig. 8a), compared to that of the corresponding $t = 0$ specimen (Fig. 4a), shows that in the former extensive destruction of the initial fibres network has occurred and the bundles of filaments appear randomly interrupted. Also the overall structure in Fig. 8a is largely covered with pulverized material which, in agreement with the IR results, is likely to represent the physical form of the hydrolytic cleavage product of the initial long fibres. At the end of the test period some of this material, which was found suspended in the alkali, was recovered and exhibited IR features similar to those of the $t = 2700$ h cardboard ($A_{955}/A_{3662} \leqslant 1.0$).

The morphological and chemical structure changes shown above did not fail to produce drastic effects on the properties. The tear point

TABLE II Comparison of plain and PPS–asbestos cardboards before ($t = 0$ h) and after ($t = 0$ h) exposure to concentrated (30 to 43 wt%) boiling KOH

Cardboard sample	KOH (wt%)	t(h)	C_i (wt%)	Weight loss (wt%)	P_t (kg cm^{-2})	Liquids regain data (wt/wt)§			A_{955}/A_{3662}**
						H_2O	Tln¶	H_2O/Tln	
Asbestos		0	0.0		30	0.44	0.38	1.17	2.01 ± 0.14
	43	104	0.0	14.9		0.82	0.68	1.21	0.69
	30	2700	0.0	32.2		0.86	0.59	1.45	0.58
Asbestos–PPS		0	6.8		68	0.22	0.37	0.59	2.01 ± 0.14
	30	2700	5.1*	9.8	17	0.59	0.49	1.20	1.87
		0	11.1		84	0.17	0.35	0.48	2.01 ± 0.14
	43	200	9.0†	8.3	47	0.53	0.45	1.17	1.78
	30	2700	8.6‡	9.4	45	0.58	0.47	1.22	1.66

*†‡Average apparent concentration calculated from R_1 and R_2 (see text) IR data: *C_i 5.0 and 5.2, †C_i 8.8 and 9.2, ‡C_i 8.1 and 9.2 from R_1 and R_2, respectively.
§g of sorbed liquid/g of dry cardboard.
¶Toluene.
**IR net (see text) absorbance ratios.

pressure of the damaged plain asbestos could not be measured due to the perforation of this material. The liquid regains (Table II) rise up to 100% of the initial $t = 0$ h values. Also the sorbed water to toluene ratio in the damaged asbestos ($X = 1.45$) is higher than that in the $t = 0$ h specimen ($X = 1.17$) and appears in agreement with the IR indication that the chemical structure of the former has become more hydrophilic due to the higher MOH/SiOSi concentration ratio. The PPS–asbestos materials on the contrary did not exhibit any visible damage at the end of the test period in the alkali. The total weight losses (9 to 10% in Table II) were considerably lower than those (15 to 32%) of the plain cardboards. The MOH/SiOSi IR absorbance ratios (lowest value = 1.66) were by far higher than those (0.60 to 0.70) of the $t > 0$ h plain asbestos cardboards although the former lowest is sligthly below the lower 95% confidence limit of the initial value (2.01) at $t = 0$ h. Accordingly the respective SiO_2 and MgO concentrations (Table I) in the $t = 2700$ h PPS–asbestos specimen were slightly lower and higher than in the $t = 0$ h cardboards; the excess of MgO over the $Mg_3Si_2O_5$ composition indicates that some leaching of silicon has occurred during the exposure of the sample to the alkali. Perhaps some loss of PPS from the cardboard takes place too; in the $t > 0$ h PPS specimen, the PPS concentrations (5.1 to 9.0), calculated from the R_1 and R_2 relative absorbances with the aid of Equations 2 and 3, result lower than the initial $t = 0$ h values (6.8 to 11.1). However the change of the A_{955}/A_{3662} ratio (due to the chemical composition change) in the host reference material may imply a change in the relative IR extinction coefficients (a_1 and a_2) of Equations 2 and 3 and thus make uncertain the $t = 2700$ h calculated C_1 values. All together the data indicate that the extent of the hydrolytic attack on the PPS–asbestos cardboard by the alkali is slight and much lower than that on the plain cardboard. The SEM micrographs of the $t = 2700$ h former material (Figs. 8c and d) confirm no visible (or very limited) damage to the coated fibres bundles (i.e. the bundle of long fibres is largely present and any pulverized material can hardly be detected). Due to the 10 wt% material loss the overall structure in Figs. 8c and d seems, however, less compact than the initial structure in Fig. 4b. The effect of these structural changes on properties (Table II) are the decrease of mechanical strength, the increase of the liquids' uptake, but, most interesting, the rise in the sorbed water to toluene ratio from the initial 0.5 to 0.6 value to 1.2. This last fact indicates that the overall HLB of the material has changed due to the formation of a more hydrophylic structure. Indeed the A_{955}/A_{3662} ratio (Table I) in the $t = 2700$ h PPS–asbestos specimen indicate that, as a consequence of the partial hydrolytic cleavage (possibly of uncoated filaments; see Fig. 4b), the relative concentration of OH functions in the polysilicate structure of the host matrix increases. The extent of this phenomenon is much more limited in the PPS–asbestos material than in plain asbestos.

Also as long as the dimensional stability and mechanical strength is sufficiently retained, a certain increase of hydrophylic functional groups (e.g. OH) in the cardboard appears mostly desirable in connection to its application as separator in alkaline water electrolysis. Fig. 9 shows that the electrical resistance of the PPS–asbestos cardboard decreases significantly after the exposure

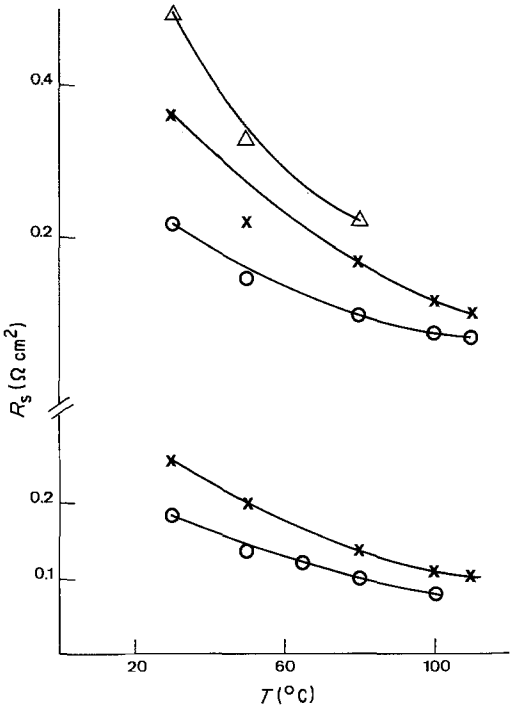

Figure 9 Electrical resistance (R_s) against temperature (T) for 0.055 cm thick asbestos cardboards. Upper and lower scales refer, respectively, to the R_s values measured in 43 and 30 wt% KOH: (○) plain and (△) 11 wt% PPS–asbestos cardboards (as made) and (×) 11 wt% PPS–asbestos cardboard after 200 to 2700 h exposure to 43 to 30% boiling KOH.

TABLE III Electrical resistance in concentrated KOH of candidate separators in advanced alkaline water electrolysis

Separator	Thickness (cm)	KOH (wt %)	T (° C)	R_s (Ω cm^2)
Porous teflon impregnated with potassium titanate [4]	0.05	28	45	0.45
Polysulphone [4]	0.18	28	45	1.08
Polytetrafluoroethylene radiografted with styrene + 5% DVB [25]		40	120	0.40

of the specimen to the potash and the electrical resistance difference between this specimen and the $t = 0$ h plain asbestos cardboard narrows down to 0.08 to 0.15 at 30° C and 0.03 Ωcm^2 at $T \geqslant 100$° C. In agreement with the liquid uptake data no significant electrical resistance difference was detected between the $t = 200$ to 2700 h samples of 6 to 10% PPS concentration.

4. Conclusions

The failure of asbestos to withstand the action of boiling concentrated alkalis has been ascribed [2] to mechanical stress induced by the formation of gas pockets into the porous structure and to the simultaneous chemical attack on the fibres by the alkali. The stabilization of asbestos has been achieved in the present work by coating its fibres with polyphenylene sulphide. This has been possible due to the availability of concentrated soaking solutions from which the organic polymer is recrystallized after penetration into the polysilicate matrix. The physisorbed organic polymer reduces the void fraction of the host material and provides increased mechanical strength and protection of the fibres from chemical attack. The action of concentrated (30 to 43 wt %) aqueous KOH is limited to minor hydrolysis of the polysilicate SiO chain bonds. This reaction does not compromise seriously the mechanical strength and dimensional stability of the cardboard but supplies the overall structure with a higher concentration of hydrophilous OH functions which increase the material wettability and lower its electrical resistance to about 0.1 Ωcm^2 at $T \geqslant 100$° C. The lack of wettability has been recognized as the main factor which in pure organic materials (e.g. polysulphones, polyphenylene sulphide and polytetrafluoroethylene [2, 4]) favours formation of gas bubbles and leads to high ohmic drop (Table III). From the comparison of the data in Table III and Fig. 9 the PPS–asbestos cardboards appear to exhibit the lowest resistance factor. This material nearly fulfils all demands to be tested in advanced alkaline water electrolysers.

Acknowledgements

This work has been sponsored by the Commission of the European Communities under contract N. EH-B/30-018-I of 1981 and EHB-34-025 I(S) of 1982. We are also grateful to Professor M. Zocchi for providing the X-ray data. The MgO and SiO_2 wet chemical analyses were performed with the technical support of Mr A. Castoldi and Miss E. Casiraghi – "Laboratorio Ufficiale di Analisi del Dipartimento di Chimica Industriale e Ingegneria Chimica del Politecnico di Milano".

References

1. T. N. VERIZOGLU, W. D. VAN VORST and J. H. KELLEY (eds), in Proceedings of the 4th WHEC, Pasadena, June 1982, Vol. 1–3 (Pergamon Press, Oxford, 1982).
2. R. RENAUD and R. L. LE ROY, *Int. J. Hydrogen Energy* 7 (1982) 155.
3. H. HOFMAN, V. PLZAK and H. WENDT, in Proceedings of the 4th WHEC, Pasadena, June 1982, Vol. 1, edited by T. N. Verizoglu, W. D. Van Vorst and J. H. Kelley (Pergamon Press, Oxford, 1982) p. 407.
4. C. T. BOWENN, B. F. HENSHAW, R. L. LE ROY and R. RENAUD, in Informal Proceedings of IEA Annex IV, Pasadena, June 1982, compiled by A. Mezzina (Brookhaven National Laboratory, Upton, New York, 1982).
5. H. W. HILL, Jr and D. G. BRADY, "Encyclopedia of Chemical Technology", Vol. 18, edited by Kirk-Othmer (J. Wiley and Sons, New York, 1982) p. 793.
6. L. GIUFFRÉ, E. MONTONERI, G. MODICA and E. TEMPESTI, in Proceedings of the 4th WHEC, Pasadena, June 1982, Vol. 1, edited by T. N. Verizoglu, W. D. Van Vorst and J. H. Kelley (Pergamon Press, Oxford, 1982) p. 319.
7. H. P. GREGOR, H. JACOBSON, R. C. SHAIR and D. M. WETSTONE, *J. Phys. Chem.* **61** (1957) 141.
8. G. MODICA, L. GIUFFRÉ, E. MONTONERI, V. POZZI and E. TEMPESTI, *Int. J. Hydrogen Energy* in press.
9. H. H. SMITH, "Encyclopedia of Polymer Science

and Technology" Vol. 10, edited by H. E. Mark and N. G. Gaylord (Interscience Publ., New York, 1969) p. 653.
10. W. C. STREIB, "Encyclopedia of Chemical Technology", Vol. 3, edited by Kirk-Othmer (J. Wiley and Sons, New York, 1982) p. 267.
11. W. NOLL, "Ullmanns Encyklopädie der Technischen Chemie", Vol. 4, edited by W. Foerst (Urban and Schwarzenberg, München, 1953) p. 40.
12. W. J. WARD III, W. R. BROWALL and R. M. SALEMME, *J. Membrane Sci.* 1 (1976) 99.
13. W. PUSCH and A. WALCH, *Angew. Chem. Int. Ed. Engl.* **21** (1982) 660.
14. W. D. BASCOM, *J. Phys. Chem.* **76** (1972) 3188.
15. O. B. BELSEEV and L. M. KISELEV, *Geol. Razved. Mestorozhd. Tverd. Polez. Iskop. Kaz.* (1968) 319.
16. J. ETCHEPARE, *Spectroch. Acta* **26A** (1970) 2147.
17. R. E. RICHARDS and H. W. THOMPSON, *J. Chem. Soc.* (1949) 124.
18. Y. TSUNAWAKI, N. IWAMOTO, T. HATTORI and A. MITSUISHI, *J. Non-cryst. Solids* **44** (1981) 369.
19. C. TOPRAK, J. N. AGAR and M. FALK, *J. Chem. Soc. Faraday Trans. I* **4** (1978) 803.
20. A. ZECCHINA, C. VERSINO, A. APPIANO and G. OCCHIENA, *J. Phys. Chem.* **72** (1968) 1471.
21. J. M. SERRATOSA and W. F. BRADLEY, *ibid.* **62** (1958) 1164.
22. R. S. McDONALD, *ibid.* **62** (1958) 1168.
23. *Idem, J. Amer. Chem. Soc.* **79** (1957) 850.
24. F. K. SCHOLL, "IR Analysis of Polymers, Resins and Additives. An Atlas", Vol. 2 (C. Hauser Verlag, München, 1973) spectrum n. 2356.
25. T. NENNER and A. FAHRASMANE, in Proceedings of the 4th WHEC, Pasadena, June 1982, Vol. 1, edited by T. N. Verizoglu, W. D. Van Vorst and J. H. Kelley (Pergamon Press, Oxford, 1982) p. 257.

Received 6 January
and accepted 18 March 1983